PROCEEDINGS OF SCIENCE

Search for Correlations of High-Energy Neutrinos with Infrared Flares in AGNs

Wenlian Li[a,b,*] **and Donglian Xu**[a,c,d]

[a] *State Key Laboratory of Dark Matter Physics, Tsung-Dao Lee Institute, Shanghai Jiao Tong University, Shanghai 201210, China*

[b] *Fakultät für Physik & Astronomie, Ruhr-Universität Bochum, 44780 Bochum, Germany*

[c] *School of Physics and Astronomy, Shanghai Jiao Tong University, Shanghai 200240, China*

[d] *Hainan Research Institute, Shanghai Jiao Tong University, Hainan, China*

E-mail: wenlianli@sjtu.edu.cn

The IceCube Neutrino Observatory issues real-time high-energy (HE) neutrino alerts and has released its first catalog (IceCat-1). However, the origin of these neutrinos remains largely unknown. Active galactic nuclei (AGNs) exhibiting variability are promising candidate sources, and previous studies have suggested temporal correlations between HE neutrino alerts and infrared (IR) flares. In this contribution, we perform a spatio-temporal correlation analysis between IceCube HE neutrino alerts and a sample of *Wide-field Infrared Survey Explorer* (WISE)-selected AGNs and radio-loud blazars, both cross-matched with the *Fermi*-LAT 4FGL-DR2 catalog. IR light curves are primarily used in the analysis, while additional γ-ray light curves are included for a subset of sources to investigate multi-band behavior. No significant correlation is found in the IR band. The most significant result appears in the γ-ray band for a subset of blazars, with a pretrial p-value of 0.05%, primarily driven by TXS 0506+056 and PKS 0446+112. However, no significant excess remains after removing these two sources. Additionally, we investigate the multi-wavelength behavior of promising candidate sources, from radio to γ-rays.

39th International Cosmic Ray Conference (ICRC2025)
15–24 July 2025
Geneva, Switzerland

*Speaker

PoS(ICRC2025)1097

1. Introduction

The IceCube Neutrino Observatory discovered a diffuse extraterrestrial neutrino flux in 2013 [1]. Compelling evidence of neutrino emission has since been found from the flaring blazar TXS 0506+056 [2, 3], the Seyfert galaxy NGC 1068 [4], and the Galactic plane [5]. However, the origins of the diffuse neutrino flux remain largely unresolved. Recently, KM3NeT detected an ultra-high-energy (UHE) neutrino event (~220 PeV) [6], whose origin also remains under debate.

Tidal disruption events (TDEs) and AGN accretion flares, both representing modes of supermassive black hole (SMBH) accretion, are promising neutrino source candidates. Several potential associations between TDEs/AGN flares and HE neutrinos have been reported, including AT2019dsg–IC191001A [7], AT2019fdr–IC200530A [8], and AT2019aalc–IC191119A [9]. All of these optically detected flares exhibited delayed IR emission, commonly interpreted as reprocessed radiation by surrounding dust—i.e., dust echoes. These IR flares align more closely with the neutrino arrival times than the optical peaks.

In the case of TDEs, neutrinos can be produced via hadronic (pp or pγ) interactions in the jet, accretion disk, corona, wind/outflow (see [10] and references therein), as well as in dust regions—for example, through interactions between UHE protons and IR photons [11]. Since AGNs share similar features, neutrino production associated with IR flares is also expected. Previous studies have searched for neutrino emission from TDE-like flares [12, 13], and no significant signals were found. In this work, we focus on a larger AGN sample and investigate potential spatio-temporal correlations between IR flares and IceCube HE neutrino alerts.

Blazars, a subclass of AGNs with jets aligned close to the line of sight, have long been studied as candidate neutrino sources. Most studies have focused on γ-ray blazars [14–17], motivated by the observed γ-ray activity of TXS 0506+056 during the detection of IC170922A [2]. However, some studies have suggested associations with lower-frequency emission. Hints of radio (and optical) flares correlated with HE neutrinos were reported in [18–20], and [21] reported a weak trend suggesting that IR flares might be temporally correlated with neutrino alerts. In a few individual cases, such as GB6 J1040+0617 (associated with IC141209A), simultaneous γ-ray and IR flaring has also been observed [14, 22].

These findings motivate a more systematic investigation of the spatial and temporal correlations between IR flares and HE neutrinos from both non-jetted and jetted AGNs (e.g., blazars). In this contribution, we construct source samples from the *Wide-field Infrared Survey Explorer* (WISE [23])-selected AGN (R90 [24]) and blazar (WIBRaLS [25, 26]) catalogs, and cross-match them with the *Fermi*-LAT 4FGL-DR2 catalog [27, 28] to identify likely variable and γ-ray-emitting sources. We perform a spatio-temporal correlation analysis using the latest IceCube alert sample (Section 2.1) and the IR light curves of Fermi-WISE blazar (FWB-IR) and Fermi-WISE AGN (FWA-IR) samples (Section 2.2). A subsample of sources with both IR and γ-ray light curves (FWB-IRγ, FWA-IRγ) is used to investigate simultaneous multi-band (IR and γ-ray) flaring behavior associated with neutrino events.

2. Multi-Messenger Sample and Data

2.1 Neutrino Data

The IceCube real-time alert system has been operational since 2016 [29]. Starting in 2019, alerts were classified into “Gold" and “Bronze" streams, corresponding to average astrophysical

purities (signalness) above 50% and 30%, respectively. In 2023, IceCube released the IceCube Event Catalog of Alert Tracks (IceCat-1 [30]), providing for each event the R.A. (α), Dec (δ), 90% uncertainty region (α^+, α^-, δ^+, δ^-), arrival time, and signalness (S).

To include the most recent data, we supplement IceCat-1 with additional "Gold" and "Bronze" alerts issued after its release, using information from the General Coordinates Network[1] (GCN) Circulars and Astrophysical Multimessenger Observatory Network (AMON) notices[2]. The resulting neutrino dataset, denoted "COMPLETE", contains 375 HE neutrino alerts from May 2011 to April 2025. It includes 340 alerts from IceCat-1[3] (8 excluded due to being induced by cosmic rays), and 35 additional alerts reported via GCN Circulars from IC231027A to IC250429A. We also define a subsample, "CUT", by requiring a 90% uncertainty region size less than 30 deg^2 [13].

2.2 Source Samples and Multi-Wavelength Data

This study uses IR-selected AGN and blazar candidates from the *WISE* AllWISE data release, including the WIBRaLS catalog [25, 26], which contains radio-loud blazar candidates with mid-IR colors similar to known γ-ray blazars, and the R90 catalog [24], which provides over 4.5 million AGN candidates selected with 90% reliability using W1 and W2 color criteria.

To refine the sample and focus on likely variable and bright sources, we apply the following cuts: (i) $S_{1.4\,\mathrm{GHz}} \geq 100$ mJy for WIBRaLS sources [21]; (ii) W1 ≤ 17 mag for R90 sources; (iii) reduced chi-square $\chi^2_{\mathrm{red}} > 1$ in both W1 and W2 bands [31], based on time-domain light curves from the *WISE* mission. These criteria yield 961 Fermi-WISE blazars (denoted FWB-IR) and 10,179 Fermi-WISE AGNs (FWA-IR), for which IR light curves are available, after spatially cross-matching with the *Fermi*-LAT 4FGL-DR2 catalog [27, 28]. The matching is based on whether a WISE source lies within the 95% error ellipse of a 4FGL-DR2 source. Since multiple WISE AGNs can fall within a single 4FGL error region, the number of matched AGNs exceeds the number of 4FGL sources, i.e., some Fermi sources have multiple possible IR counterparts.

The *WISE* IR light curves in the W1 (3.4 μm) and W2 (4.6 μm) bands are obtained using the `timewise` package[4] [31], which combines multi-epoch AllWISE and single-epoch NEOWISE-R photometry [32]. The resulting light curves span from 2010 to 2024 with a mean interval of ~180 days, except for a data gap between 2011 and 2013 due to mission transition. We require signal-to-noise ratio (S/N) > 2 and at least three detections per band.

To study γ-ray variability, we extract monthly-binned light curves from the *Fermi*-LAT Light Curve Repository (LCR) [33] for sources with a variability index ≥ 21.67, corresponding to a $< 1\%$ probability of being steady [27]. Only data points with significance $\geq 2\sigma$ are used. This results in 618 FWB and 2,473 FWA sources with both IR and γ-ray light curves, denoted as FWB-IRγ and FWA-IRγ, respectively. A summary of source catalogs, selection criteria, and sample sizes is provided in Table 1. Sample overlaps are visualized in Figure 1.

Additionally, for selected source candidates, we collect light curves across multiple wavelengths: radio/mm data from RATAN-600 [34] and ALMA calibrator catalogs [35], optical data from ATLAS forced photometry [36], and X-ray data from *Swift*-XRT [37, 38].

[1] https://gcn.nasa.gov/

[2] https://gcn.gsfc.nasa.gov/amon_icecube_gold_bronze_events.html

[3] https://doi.org/10.7910/DVN/SCRUCD

[4] https://timewise.readthedocs.io/en/latest/

Data	Catalog	Selection Criteria		Number of Sources		
		Source Criteria (1)	WISE LC Criteria (2)	Brightness cut	4FGL-DR2 matches	4FGL LCR matches
WISE IR Blazar	WIBRaLS [25, 26]	$S_{1.4\,\mathrm{GHz}} \geq 100$ mJy	$\chi^2_{\mathrm{red}} > 1$ S/N > 2	5,396	961 (FWB-IR)	618 FWB-IRγ)
WISE IR AGN	R90 [24]	Mag (W1) ≤ 17	# of detection ≥ 3	2,543,530	10,179 (FWA-IR)	2,473 FWA-IRγ)

Table 1: Source lists, selection criteria, and the final source sample used in the analyses.

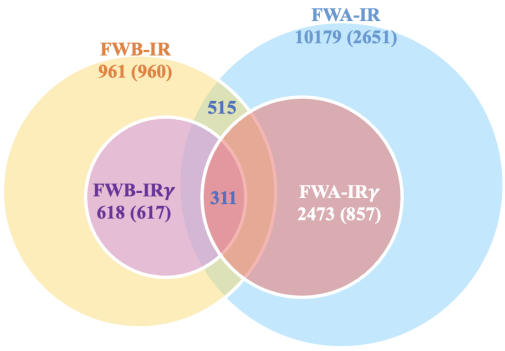

Figure 1: Source overlaps among the samples used in this analysis. Numbers outside (inside) brackets indicate the number of WISE sources (unique 4FGL-DR2 counterparts). A single 4FGL source can match multiple WISE sources within its 95% error ellipse.

3. Analysis Method

In this study, we search for correlations between IR and γ-ray flares and HE neutrino alerts from AGNs, following the methodology outlined in [18–20].

To quantify potential associations, we define five test statistics (TS): (1) Mean flux density $\overline{S}$ of associated sources. (2) Activity Index (AI), defined as the ratio of the average flux density within a time window ΔT, centered on the neutrino arrival time, to that outside the window. In this work, we adopt $\Delta T = 570$ days for the IR band and 22 days for the γ-ray band, following the optimization performed in [21]. (3) $\mathrm{AI}_{\mathrm{scaled}}$: AI scaled by the peak flux of the light curve, to account for bright flares outside ΔT that may reduce the AI. (4) $\mathrm{AI}_{0.01\%}$: Number of associated AGNs exhibiting flares at the 99.99% confidence level (i.e., AI > $\mathrm{AI}_{\mathrm{threshold}} > 1$). The thresholds are derived following the method in [20], in which the flux densities of randomly selected light curves from the source sample are randomized assuming Gaussian errors. False-AI values are then calculated as the ratio between the mean flux of the randomized and original light curves. Repeating this process 10^5 times yields a false-AI distribution, from which the 99.99% thresholds are determined: 1.10 (IR) and 1.68 (γ-ray) for the FWB-IRγ sample. (5) $N_{\mathrm{flare,BB}}$: Number of associated sources flaring at the neutrino arrival time as identified by the Bayesian Blocks algorithm [39]. We adopt the `astropy` implementation[5] to segment light curves and define flaring periods independently of AI. Following

[5] https://docs.astropy.org/en/stable/api/astropy.stats.bayesian_blocks.html

[21], a block is considered flaring if $F_{\rm block} > F_{\rm quiescent} + 1.3 \times S$ and $F_{\rm block} > F_{\rm avg} + S$, where $F_{\rm block}$ is the mean flux in the block, $F_{\rm quiescent}$ is the mean of the faintest ~30% of data points, and S is the standard deviation.

Each TS is computed for all AGN–neutrino association pairs. Global TS values are then derived: $\overline{S}$, AI, and $\mathrm{AI_{scaled}}$ are averaged over all sources within the 90% uncertainty region, while $\mathrm{AI_{0.01\%}}$ and $N_{\rm flare,BB}$ count the number of sources exceeding thresholds and flaring at the neutrino arrival time. For the COMPLETE neutrino sample, a weighting scheme is applied when deriving global TS values to mitigate the effects of multiple associations from alerts with large 90% uncertainty regions:

$$W = S \cdot \widetilde{\Omega}/\Omega, \tag{1}$$

where S is the signalness, Ω is the 90% uncertainty region size, and $\widetilde{\Omega}$ is its global median.

For the FWA/FWB-IR samples, the analysis is based solely on IR light curves. For the FWA/FWB-IRγ samples, three scenarios are explored: (1) IR only, (2) γ-ray only, and (3) combined IR + γ-ray analysis. In the combined IR + γ-ray analysis, $\overline{S}$, AI, and $\mathrm{AI_{scaled}}$ are averaged across both bands, while $\mathrm{AI_{0.01\%}}$ and $N_{\rm flare,BB}$ count only sources flaring in both bands simultaneously. For AI-related TS parameters, associations are omitted if the AI value cannot be determined due to missing data within the selected time window.

To assess the significance of the spatio-temporal correlation, we perform Monte Carlo simulations by randomizing the R.A. of each alert to generate the background TS distribution. The p-value, representing the chance coincidence probability, is calculated as [40]:

$$p = \frac{M+1}{N+1}, \tag{2}$$

where M is the number of random trials with TS greater than the observed value ($TS_{\rm obs}$), i.e., $M = \sum_i [TS_i > TS_{\rm obs}]$, and $N = 10^5$ is the total number of random realizations.

4. Results and Discussion

Since there are overlaps between source samples, we present results for the smallest sample (FWB-IRγ) and the largest sample (FWA-IR). The pretrial p-values obtained using the CUT (unweighted) and COMPLETE (weighted) neutrino samples are summarized in Table 2 and Table 3, respectively.

Sample	**Bands**	$\overline{S}$	AI	$\mathrm{AI_{scaled}}$	$\mathrm{AI_{0.01\%}}$	$N_{\rm flare,BB}$
FWB-IRγ	IR	0.049	0.014	0.052	0.93	0.64
	γ-ray	0.21	5.0×10^{-4}	0.13	0.19	0.074
	IR + γ	0.051	0.0028	0.080	0.33	0.26
FWA-IR	IR	0.37	0.38	0.25	0.74	0.35

Table 2: Pretrial p-values obtained from five TS parameters using the CUT neutrino sample.

While no significant correlation is found in the IR band, the most significant result arises from the FWB-IRγ sample using AI as the TS in the γ-ray band (CUT sample), with a pretrial p-value of 5.0×10^{-4}. The two strongest correlations—i.e., the blazar–neutrino pairs with the highest AI

Sample	**Bands**	$\overline{S}$	AI	$\mathrm{AI_{scaled}}$	$\mathrm{AI_{0.01\%}}$	$N_{\mathrm{flare,BB}}$
FWB-IRγ	IR	0.093	0.56	0.089	0.85	0.16
	γ-ray	0.28	0.030	0.15	0.040	0.032
	IR + γ	0.11	0.29	0.14	0.17	0.057
FWA-IR	IR	0.85	0.71	0.64	0.84	0.16

Table 3: Pretrial p-values obtained from five TS parameters using the COMPLETE neutrino sample, with a weighting scheme applied.

values—are TXS 0506+056–IC170922A and PKS 0446+112–IC240105A, with corresponding AI values of 4.36 and 3.04 in the γ-ray band, respectively. Removing TXS 0506+056 (or both sources) from the analysis reduces the significance, yielding a p-value of 0.015 (1.0).

PKS 0446+112 (also know as 4FGL J0449.1+1121 or J044907.67+112128.6) is a distant blazar at redshift $z = 2.153$, classified as intermediate between a flat-spectrum radio quasar (FSRQ) and a BL Lac object [41]. Around the arrival time of IC240105A (a "Bronze" alert [42]), PKS 0446+112 showed enhanced activity across multiple wavelengths, as illustrated in Figure 2. Notably, PKS 0446+112 exhibits characteristics of a low-energy synchrotron peak BL Lac object (LBL). While some studies have suggested that intermediate- and high-energy-peaked blazars (IBLs and HBLs) are more likely to be associated with HE neutrinos, no such excess has been found for LBLs [17].

Some previously reported blazars are not included because the associated alert is not part of IceCat-1 (e.g., GB6 J1040+0617, associated with IC141209A), or because the source does not exhibit significant IR or γ-ray flaring activity at the neutrino arrival time (e.g., PKS 1502+106, associated with IC190730A).

The AI-based TS parameters (AI, $\mathrm{AI_{scaled}}$, $\mathrm{AI_{0.01\%}}$) depend on the choice of the time window. In this study, we adopt values from previous blazar–neutrino analyses [21]. Since our sample includes both blazars and non-blazar AGNs, future work will consider optimized or source-specific time windows. Additionally, we will investigate the multi-wavelength behavior of AGNs with strong IR flares (high AI values) and evaluate the sensitivity of our analysis across different subsamples.

Acknowledgements

This work has received support from the National Natural Science Foundation of China (No. 12175137).

References

[1] **IceCube** Collaboration, M. G. Aartsen *et al.* *Science* **342** (2013) 1242856.

[2] **IceCube** Collaboration, M. G. Aartsen *et al.* *Science* **361** no. 6398, (2018) eaat1378.

[3] **IceCube** Collaboration, M. G. Aartsen *et al.* *Science* **361** no. 6398, (2018) 147–151.

[4] **IceCube** Collaboration, R. Abbasi *et al.* *Science* **378** no. 6619, (2022) 538–543.

[5] **IceCube** Collaboration, R. Abbasi *et al.* *Science* **380** no. 6652, (2023) adc9818.

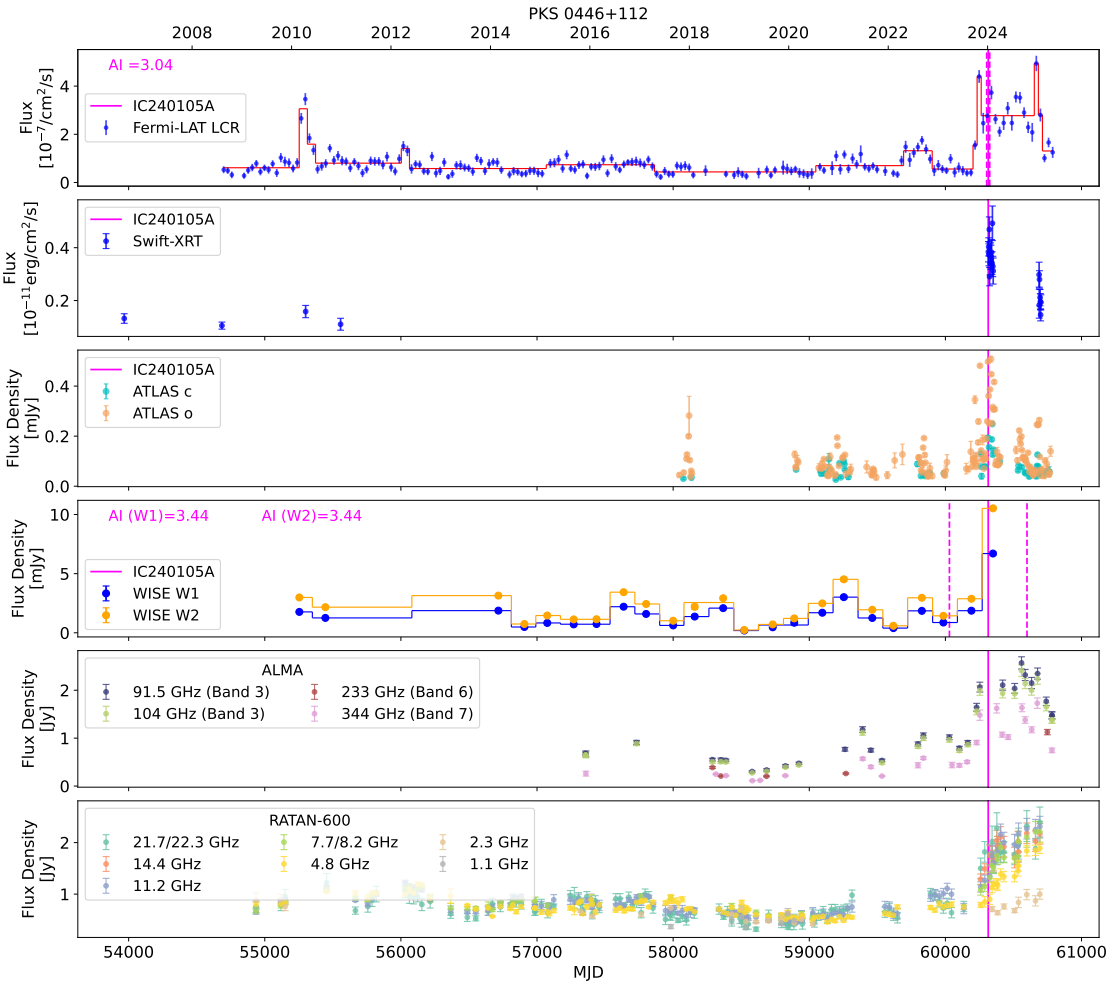

Figure 2: Multi-wavelength light curve of PKS 0446+112. The solid magenta line indicates the arrival time of the high-energy neutrino IC240105A. The dashed magenta line marks the time window centered on the neutrino arrival time, i.e., $\pm\Delta T/2$, where ΔT is 570 days for the IR band and 22 days for the γ-ray band.

[6] **KM3NeT** Collaboration, S. Aiello *et al.* *Nature* **638** no. 8050, (2025) 376–382. [Erratum: Nature 640, E3 (2025)].

[7] R. Stein *et al.* *Nature Astron.* **5** no. 5, (2021) 510–518.

[8] S. Reusch *et al.* *Phys. Rev. Lett.* **128** no. 22, (2022) 221101.

[9] S. van Velzen *et al.* *Mon. Not. Roy. Astron. Soc.* **529** no. 3, (2024) 2559–2576.

[10] K. Hayasaki *Nature Astron.* no. 5, (2, 2021) 436–437.

[11] W. Winter and C. Lunardini *Astrophys. J.* **948** no. 1, (2023) 42.

[12] **IceCube** Collaboration, R. Abbasi *et al.* *PoS* **ICRC2023** (2023) 1478.

[13] M.-X. Lu, Y.-F. Liang, X.-G. Wang, and X.-R. Ouyang.

[14] **Fermi-LAT, ASAS-SN, IceCube** Collaboration, S. Garrappa *et al.* *Astrophys. J.* **880** no. 2,

(2019) 880:103.

[15] A. Franckowiak *et al.* *Astrophys. J.* **893** no. 2, (2020) 162.

[16] **IceCube** Collaboration, R. Abbasi *et al.* *Astrophys. J.* **954** no. 1, (2023) 75.

[17] P. Giommi, T. Glauch, P. Padovani, *et al.* *MNRAS* **497** no. 1, (2020) 865–878.

[18] A. Plavin, Y. Y. Kovalev, Y. A. Kovalev, and S. Troitsky *Astrophys. J.* **894** no. 2, (2020) 101.

[19] T. Hovatta *et al.* *Astron. Astrophys.* **650** (2021) A83.

[20] P. M. Kouch *et al.* *Astron. Astrophys.* **690** (2024) A111.

[21] Y.-L. Chang, B. Arsioli, W. Li, D. Xu, and L. Chen *Astrophys. J.* **939** no. 2, (2022) 123.

[22] K. É. Gabányi, S. Frey, and A. Moór *Res. Notes AAS* **3** no. 2, (Feb., 2019) 36.

[23] E. L. Wright *et al.* *Astron. J.* **140** (2010) 1868.

[24] R. J. Assef, D. Stern, G. Noirot, *et al.* *Astrophys. J. Suppl.* **234** no. 2, (2018) 23.

[25] R. D'Abrusco, F. Massaro, A. Paggi, *et al.* *Astrophys. J. Suppl.* **215** no. 1, (2014) 14.

[26] R. D'Abrusco *et al.* *Astrophys. J. Suppl.* **242** no. 1, (2019) 4.

[27] **Fermi-LAT** Collaboration, J. Ballet, T. H. Burnett, S. W. Digel, and B. Lott.

[28] **Fermi-LAT** Collaboration, S. Abdollahi *et al.* *Astrophys. J. Suppl.* **247** no. 1, (2020) 33.

[29] **IceCube** Collaboration, M. G. Aartsen *et al.* *Astropart. Phys.* **92** (2017) 30–41.

[30] **IceCube** Collaboration, R. Abbasi *et al.* *Astrophys. J. Suppl.* **269** no. 1, (2023) 25.

[31] J. Necker, E. Graikou, M. Kowalski, *et al.* *Astron. Astrophys.* **695** (2025) A228.

[32] A. Mainzer, J. Bauer, R. M. Cutri, *et al.* *Astrophys. J.* **792** no. 1, (Aug, 2014) 30.

[33] **Fermi-LAT** Collaboration, S. Abdollahi *et al.* *Astrophys. J. Suppl.* **265** no. 2, (2023) 31.

[34] M. G. Mingaliev, Y. V. Sotnikova, R. Y. Udovitskiy, *et al.* **572** (Dec., 2014) A59.

[35] M. Bonato, E. Liuzzo, D. Herranz, *et al.* **485** no. 1, (May, 2019) 1188–1195.

[36] J. L. Tonry, L. Denneau, A. N. Heinze, *et al.* **130** no. 988, (June, 2018) 064505.

[37] P. A. Evans, A. P. Beardmore, K. L. Page, *et al.* **469** no. 1, (July, 2007) 379–385.

[38] P. A. Evans, A. P. Beardmore, K. L. Page, *et al.* **397** no. 3, (Aug., 2009) 1177–1201.

[39] J. D. Scargle, J. P. Norris, B. Jackson, and J. Chiang *Astrophys. J.* **764** (2013) 167.

[40] A. C. Davison and D. V. Hinkley, *Bootstrap methods and their application*. No. 1. Cambridge university press, 1997.

[41] S. Paiano, R. Falomo, A. Treves, R. Scarpa, and B. Sbarufatti *Astrophys. J.* **968** (2024) 81.

[42] IceCube Collaboration *GCN* **35498** (Jan., 2024) 1.